# Molecular organization and structural stability of .beta.s-crystallin from calf lens

**ARTICLE** *in* BIOCHEMISTRY · APRIL 1990

Impact Factor: 3.02 · DOI: 10.1021/bi00468a020



**3 AUTHORS:**

Paola Stiuso
Second University of Naples
**82** PUBLICATIONS **813** CITATIONS
SEE PROFILE

Raffaele Ragone
Second University of Naples
**97** PUBLICATIONS **1,239** CITATIONS
SEE PROFILE

Giovanni Colonna
Second University of Naples, Naples, Italy
**225** PUBLICATIONS **2,638** CITATIONS
SEE PROFILE

Meister, A., & Anderson, M. (1983) *Annu. Rev. Biochem. 52*, 711–760.
Shames, S. L., Fairlamb, A. H., Cerami, A., & Walsh, C. T. (1986) *Biochemistry 25*, 3519–3526.
Shim, H., & Fairlamb, A. H. (1988) *J. Gen. Microbiol. 134*, 807–817.
Stadtman, E. R., & Ginsburg, A. (1974) *Enzymes (3rd Ed.) 10*, 755–807.
Tabor, H., & Tabor, C. W. (1975) *J. Biol. Chem. 250*, 2648–2654.
Tabor, C. W., & Tabor, H. (1984) *Annu. Rev. Biochem. 53*, 749–790.

# Molecular Organization and Structural Stability of $\beta_s$-Crystallin from Calf Lens†

Paola Stiuso, Raffaele Ragone, and Giovanni Colonna*
*Chair of Chemistry, Department of Biochemistry and Biophysics, University of Naples, Via Costantinopoli 16, 80138 Naples, Italy*

*Received July 25, 1989; Revised Manuscript Received December 14, 1989*

ABSTRACT: $\beta_s$-Crystallin has been purified to homogeneity. Its structural features and conformational behavior have been studied in solution. Protein secondary structure was estimated by curve fitting of far-UV circular dichroism spectra, which gave 16% $\alpha$-helix, 45% $\beta$-sheet, 12% bends, and 27% remainders. This result indicates that the structural organization of $\beta_s$-crystallin is reasonably similar to that of other $\beta$ and $\gamma$ family members. A comparison assessed between $\beta_s$- and $\gamma_2$-crystallin by the use of predictive methods (flexibility and volume plots) reveals that the two proteins differ in respect to their local flexibility and packing, although they show similar overall organization. The interdomain and the C-terminal regions were found to be more flexible in $\beta_s$-crystallin. This finding can be explained by the presence of smaller amino acid residues within these structural districts. The location of one out of four tryptophans, i.e., Trp-162, in a flexible and exposed region of the protein was found to be the origin of the fluorescence heterogeneity. In fact, the fluorescence emission maximum of the native protein, centered at 328 nm, is due to two emitting centers, whose emission maxima are located at 323 and 330 nm, respectively, as evidenced by acrylamide quenching of fluorescence. The effect of perturbing agents, such as pH and guanidine hydrochloride, on the conformational behavior of $\beta_s$ has also been evaluated by numerous spectroscopic techniques. The range of pH stability was between 6.5 and 8. Above this interval, a conformational change takes place. In the acid region, the protein is unstable and precipitates irreversibly. The conformational resistance to guanidine hydrochloride has also been shown to be weak. GdnHCl denaturation curves were neither superimposable nor ascribable to a very cooperative transition. This result suggests a non-two-state denaturation equilibrium reflecting the presence of structural domains. The main conclusion of our work is that the protein shows a very narrow range of stability. This result indicates that an inherent structural stability may not be a general property of lens proteins. Therefore, the evolutive hypothesis about a specific recruitment of stable proteins in the lens architecture may need reconsideration.

The eye lens is remarkable for its high protein content (Lindley et al., 1985). It is organized in a complex supramolecular system, responsible for the lens optical properties. The lens can thus be considered a real "proteic" lens, whose supramolecular structure is a tridimensional network of proteins. Their role and function are still barely known. The main fraction of these proteins is represented by the "crystallins", a group formed by three major species of proteins designated as $\alpha$-, $\beta$-, and $\gamma$-crystallins (Lindley et al., 1985). These proteins are believed to act as the primary determinant of the lens tissue's optical properties (e.g., transparency, refractive index, optical anisotropy, etc.), but no biological activity has been associated with them. Of course, numerous other minor protein species are also present in the lens, such as some enzymes, membrane proteins, filamentous proteins, etc. (Alcala & Maisel, 1985). No clear data are available regarding the relative distribution and role of different proteins within the supramolecular network of the normal lens. Only recently, systematic and detailed structural studies of each proteic component of normal lens have begun [e.g., see Tardieu et al. (1986), Mandal et al. (1987), and Wistow et al. (1983)].

The $\beta$ fraction is composed of $\beta_L$ (organized in dimers and trimers) and of $\beta_H$ (organized in higher aggregates) components (Siezen & Argos, 1983). The $\gamma$ fraction is composed of several low molecular weight monomeric isoproteins (Pulcini et al., 1989), the biosynthesis of which is modulated during the differentiation (Slingsby & Croft, 1973; Slingsby & Miller, 1983; Siezen et al., 1985). $\beta_s$ is a very peculiar minor component of the $\beta$ fraction, since it is the only monomeric low molecular weight soluble protein of this fraction (Lindley et al., 1985). $\beta$- and $\gamma$-crystallins form a superfamily of related proteins, which are likely derived from a common gene (Wistow et al., 1981). They have been found to be homologous by sequence analysis. This finding is very interesting because only the $\gamma_2$ structure is known at the X-ray level (Wistow et al., 1983). The possible organization of the common structural unit shared by $\beta$ and $\gamma$ family members should be a four-motif $\beta$-barrel structure (Quax-Jeuken et al., 1985). We have focused our attention on $\beta_s$, the molecular properties of which are still unknown. This protein resembles $\gamma$ components as far as solubility, molecular weight, and monomeric structure are concerned, but it is classically classified into the $\beta$ fraction.

† This work was supported by grants from the Italian Ministry of Education (MPI 40% and 60%).
* To whom correspondence should be addressed.

0006-2960/90/0429-3929$02.50/0 

We believe that it will be extremely difficult to suggest a reliable, although simple, working model of the normal eye lens without a rigorous knowledge of the structural properties and conformational behavior of all lens proteins in solution. The knowledge of the normal lens organization will also shed light on the molecular mechanism of eye pathology. The structural organization of $\beta_s$-crystallin shows some similarities with $\gamma_2$-crystallin, but the results indicate a very narrow range of conformational stability. The protein is stable only around neutrality (pH 6.5–8) and badly suffers from denaturant action. Numerous other structural features, such as fluorescence heterogeneity, domain organization, and behavior in solution, have been clarified. Nevertheless, it still remains to be explained why this protein must possess such a limited range of stability.

## Materials and Methods

*$\beta_s$-Crystallin.* Eyes of 4–5-month-old calves were obtained from a local slaughterhouse. Only completely clear and nonpathological specimens were decapsulated and denucleated. The cortical tissue was homogenized in 5 volumes of ice-cold 0.1 M tris(hydroxymethyl)aminomethane hydrochloride (Tris-HCl),[1] 0.15 M KCl, and 0.01 M $\beta$-mercaptoethanol buffer (pH 7.5). Unless otherwise stated, the following operations were carried out at 4 °C. All solutions were degassed and carefully saturated with nitrogen to minimize oxidation phenomena.

The $\gamma$ fraction was essentially prepared according to the method of Björk (1964). $\beta_s$-Crystallin was separated from the whole $\gamma$-crystallin by DEAE (Van Dam, 1966). The protein appeared to be homogeneous when tested by SDS–PAGE by showing a single band of $M_r$ 20 000.

*Protein Concentration.* Spectrophotometric determination of $\beta_s$-crystallin concentration was performed by using $\epsilon_{280} = 3.78 \times 10^4$ $M^{-1} \cdot cm^{-1}$. This value was calculated by the content of aromatic residues in the sequence of $\beta_s$ according to Wetlaufer (1962). The protein samples under spectroscopic investigation were always dialyzed against numerous changes of buffer, which was used as a blank for the measurements.

*Spectral Measurements.* Fluorescence measurements were always made in the range of fluorescence linearity. The absorbance of all solutions was about 0.1 ODU at the excitation wavelength. The temperature of the solution cell was maintained at 22 °C. Polarization measurements were performed on a Perkin-Elmer MPF44B spectrofluorometer. The polarization was calculated by $P = (I_{vv} - GI_{vh})/(I_{vv} + GI_{vh})$, where $G = I_{hv}/I_{hh}$, $I$ is the intensity, and the first and the second subscripts refer to the plane of polarization of the excitation and emission beams, respectively, i.e., V, vertical, and H, horizontal.

Circular dichroism measurements were carried out on a Jobin Yvon Mark III spectropolarimeter equipped with a temperature-controlled cell holder. The molar ellipticity, in units of degrees centimeter squared per decimole, was calculated by using a value of 115 as the mean residue molecular weight.

The circular dichroism spectra in the spectral region between 200 and 240 nm were analyzed to evaluate the amount of secondary structure. A computerized program with five different methods of analysis (Menéndez-Arias et al., 1989) was used.

*Predictive Methods.* Plots were generated by a routine of the program FAST, version 1.1 (Facchiano et al., 1989). A seven-residue shifting window was used along the protein sequences. Three properties of amino acid residues were utilized. Bulk hydrophobicities calculated by Manavalan and Ponnuswamy (1978) were chosen for taking into account preferential hydrophobic microenvironments in proteins (Rose et al., 1985). The volume of amino acid residues in protein crystals was used as proposed by Chothia (1984). Flexibilities of amino acid residues were used as proposed by Ragone et al. (1989). The threshold value (1300) in the flexibility plots corresponds to the product between the normalized values of the highest hydrophobicity and the largest volume among turn-inducing residues, according to Ragone et al. (1989). Pseudotridimensional plots were generated as described by Facchiano et al. (1988). Net charge plots were performed with a seven residue shifting window by the GENEPRO program, version 4.1 (by Hoefer Scientific Instruments).

*Chemicals and Solutions.* Spectroscopic-grade guanidine hydrochloride was from Schwarz/Mann. All chemicals were reagent grade and were purchased from British Drug Houses. In denaturation experiments, the protein was added to buffered solutions of GdnHCl; 0.15 M KCl was present in all solutions. The fluorescence was then followed until an apparent equilibrium was reached.

Alkaline titration was performed in a special cell by careful addition of small amounts of KOH to buffered solutions (0.05 M Tris/0.15 M KCl) from an Agla syringe. The solution cell was continuously stirred and fluxed by a stream of pure $N_2$. pH measurements were carried out by using combination electrodes with a Radiometer Model 26 pH meter.

## Results

The amino acid sequence (Quax-Jeuken et al., 1985) of $\beta_s$-crystallin was analyzed by several predictive methods to yield structural information useful in the analysis of the protein organization in solution.

In Figure 1A, the hydrophobicity plots (Manavalan & Ponnuswamy, 1978; Rose et al., 1985) of both $\beta_s$- and $\gamma_2$-crystallin are reported. We compared these proteins since their sequence homology and some evolutive relationships (Quax-Jeuken et al., 1985) strongly suggest that they have similar structural organization. The two sequences were paired on the deep minimum they show at position 88 (83 for $\gamma_2$). This would correspond to the interdomain connecting segment (Wistow et al., 1983). The coupling allows a five-residue shift in the N-terminal region of $\beta_s$-crystallin compared to that of $\gamma_2$-crystallin.

The comparison shows a strong similarity between the two plots. This should reflect a similar general architecture of the two proteins. It strongly confirms the hypothesis that $\beta_s$ and $\gamma_2$ are structurally related and that they consist of two folding units or domains (Wistow et al., 1983; Quax-Jeuken et al., 1985). We also evaluated local flexibilities possessed by these proteins by using our flexibility plot recently set up by us (Ragone et al., 1989). This analysis introduces the balanced effect of amino acid volumes and hydrophobicities to extract flexibility information. Therefore, local flexibilities and packing differences of two similar structures can be promptly shown.

In Figure 1B, a comparison of plots reveals that two molecular regions show local flexibility differences despite the strong similarity found according to hydrophobicity criteria. In fact, 75–105 and 145–170 segments of $\beta_s$-crystallin are more flexible (or less rigid) than the corresponding counterparts of $\gamma_2$. The 75–105 region is involved in the interdomain con-

[1] Abbreviations: amino acids are indicated by the three-letter code; CD, circular dichroism; GdnHCl, guanidine hydrochloride; SDS–PAGE, sodium dodecyl sulfate–polyacrylamide gel electrophoresis; UV, ultraviolet; Tris-HCl, tris(hydroxymethyl)aminomethane hydrochloride; $M_r$, molecular weight.

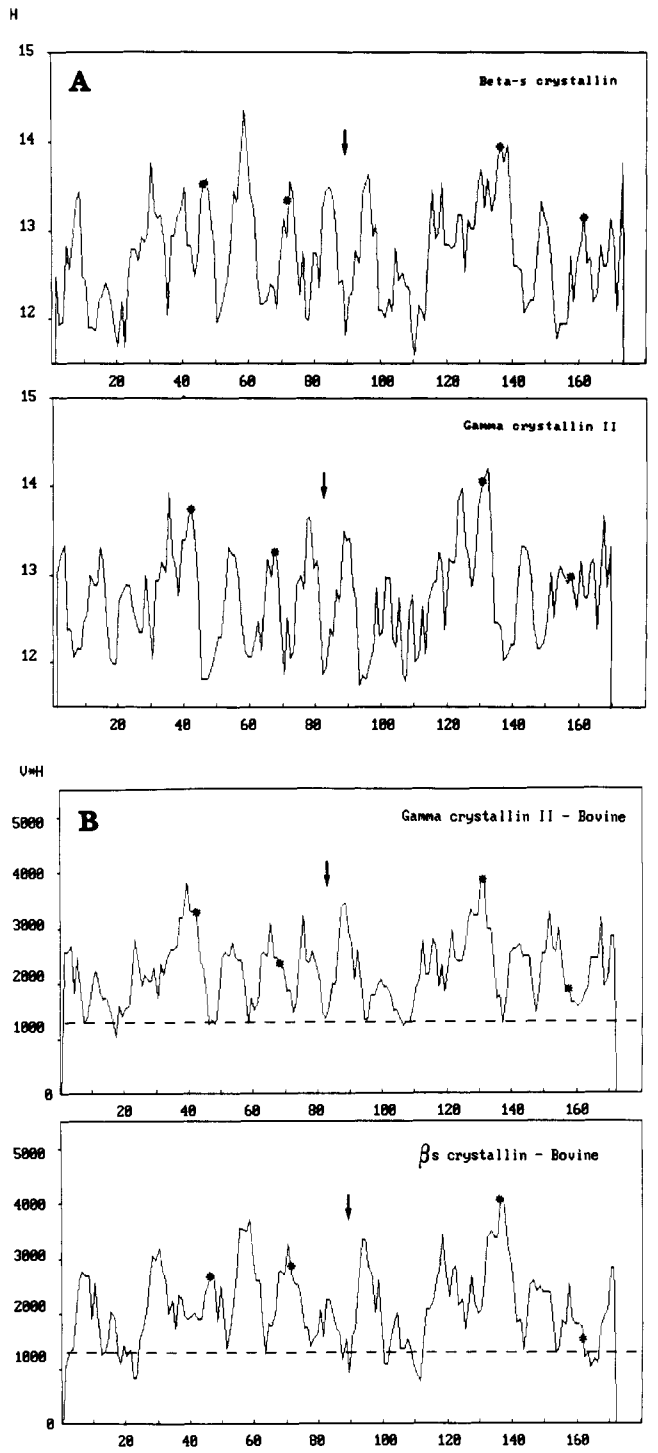


FIGURE 1: (A) Hydrophobicity plots of $\beta_s$- and $\gamma_2$-crystallin. The arrow indicates the interdomain segment, the position of which was used to normalize the sequences. Asterisks indicate the position of tryptophans along the sequence. (B) Flexibility plots of $\beta_s$- and $\gamma_2$-crystallin. Arrows and asterisks as in (A). The dashed line indicates the threshold value as suggested by Ragone et al. (1989).

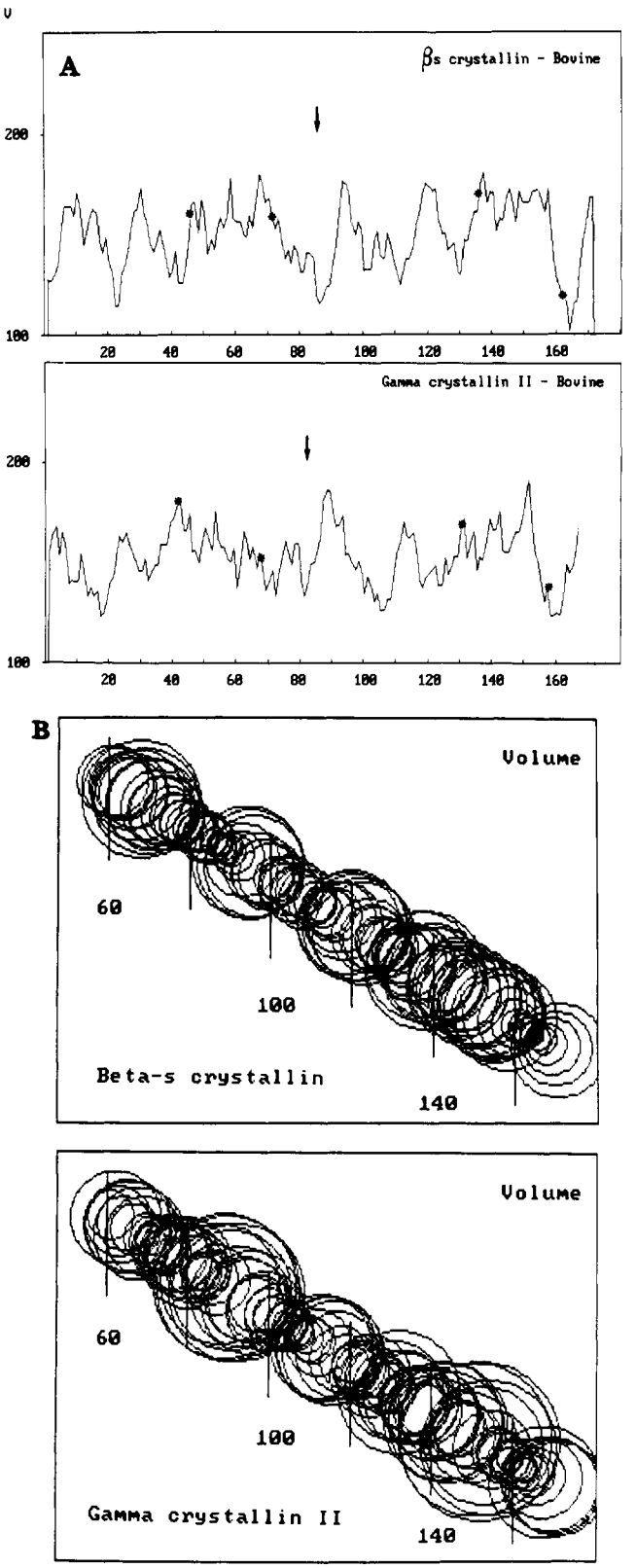


FIGURE 2: (A) Volume plots of $\beta_s$- and $\gamma_2$-crystallin. Arrows and asterisks as in Figure 1. (B) Pseudotridimensional representation of volume plots for $\beta_s$- and $\gamma_2$-crystallin according to Facchiano et al. (1988). Plots show sequence segments from 60 to the end.

nection (Wistow et al., 1983; Summers et al., 1984a), while the 145–170 segment is located in the end part of the C-terminal domain. The explanation of these differences comes from volume plots of the two proteins (Figure 2A). One can observe that these regions of $\beta_s$ show lower values of volume profile in respect to the corresponding ones of $\gamma_2$. They reflect a less rigid packing due to the diffuse presence of less voluminous residues. Figure 2B shows a pseudotridimensional representation (Facchiano et al., 1988) of the volume plots. The graph allows a quick visual check of the packing differences between $\beta_s$- and $\gamma_2$-crystallin. These segments should possess the best structural and thermodynamic requirements supporting an increase of the local flexibilities (Rose et al., 1985; Ragone et al., 1989). Their minor volume stabilizes the organized structure by increasing the local flexibility. This effect is a consequence of a diminished loss of local conformational entropy as well as a reduced exposed surface (Ragone et al., 1989). Therefore, the difference of local volumes may

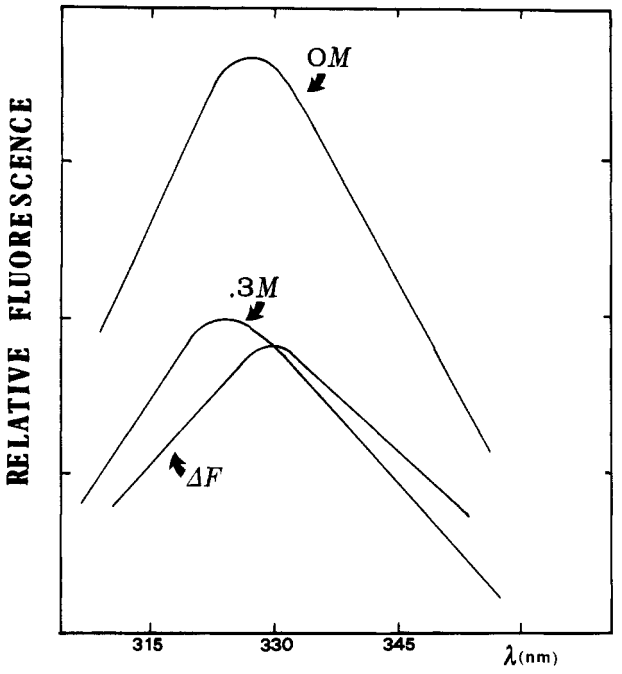


FIGURE 3: Fluorescence spectra (excitation at 295 nm) of native $\beta_s$ at pH 7.0 in 0.05 M phosphate and 0.15 M KCl in the presence of 0.3 M acrylamide. The difference spectrum ($\Delta F = F_{350} - F_{330}$ nm) is reported at the bottom.

be considered the structural ground of the enhanced flexibility.

We have also attempted an analysis of microenvironmental features possessed by tryptophan residues in $\beta_s$. Tryptophans are located at positions 46, 72, and 136, embedded in an apolar but also very rigid protein matrix. Tryptophan-162 is in a very flexible site of the C-terminal segment, where it has high probability of being partially exposed to solvent.

The fluorescence spectrum of $\beta_s$-crystallin is reported in Figure 3. It is well-known that the emission maximum wavelength of protein fluorophores is mainly affected by their microenvironmental polarity. In the neutral pH region, the emission maximum of $\beta_s$-crystallin is centered at 328 nm (excitation at 295 nm), which indicates that tryptophanyl residues are embedded in a relatively hydrophobic environment. The same evidence arises from the shoulder at 292 nm, which is present in the absorption spectrum (not shown). We investigated the fluorescence heterogeneity of tryptophan (Irace et al., 1981) in $\beta_s$-crystallin by using acrylamide as a quencher of tryptophan fluorescence (Eftink & Ghiron, 1976). The quenching efficiency of acrylamide is mainly directed against exposed tryptophanyl residues (Eftink & Ghiron, 1976; Lehrer & Leavis, 1978) so that the residual fluorescence is prevalently from buried residues. Figure 3 also shows that the fluorescence emission of the native protein is partially quenched by 0.3 M acrylamide. The emission maximum undergoes a 5-nm shift to the blue, thus occurring at 323 nm, which is characteristic of deeply buried residues. The resulting difference spectrum, i.e., native minus 0.3 M acrylamide fluorescence, has a maximum located at about 331 nm. Thus, tryptophanyl residues of $\beta_s$-crystallin do not appear to be equivalent, because their emission maxima are centered at different wavelengths. This result agrees well with the structural location of tryptophans in $\beta_s$-crystallin as estimated by the sequence analysis reported in Figure 1. In fact, three out of four tryptophans are located in very hydrophobic sites of the protein. The last one is in a more hydrophilic environment.

The far-ultraviolet CD spectra of $\beta_s$-crystallin at two different pHs are presented in Figure 4. The optical activity

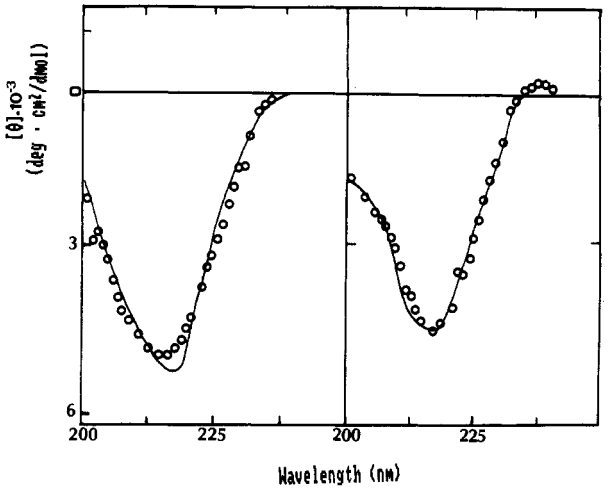


FIGURE 4: Far-UV CD spectra of $\beta_s$ at pH 7 (left) and 9.5 (right). Circles indicate the computed curves which best fit the experimental CD spectra; the estimated amounts of secondary structure are reported in Table I.

Table I: Relative Amounts of Secondary Structure of $\beta_s$-Crystallin under Various Experimental Conditions

| condition | $N$ | α-helix (%) | β conformation (%) | β-turns (%) | remainder (%) | rms[c] |
|---|---|---|---|---|---|---|
| pH 7.0[a,b] | 4 | 16 | 45 | 12 | 27 | 8 |
| pH 9.5[a] | 3 | 19 | 52 | 5 | 24 | 9 |

[a] Amount of secondary structure determined by fit according to Chang (1978). [b] The secondary structure content, as determined by sequence, according to Chou and Fasman (1974a,b, 1978), was found to be $\alpha$ = 20%, $\beta$ = 31%, turns = 35%, and remainder = 14%. [c] Normalized root mean square error of the fit (Brahms & Brahms, 1980).

of the peptide chromophore in the far-UV is remarkably sensitive to the structural organization of the polypeptide chain. The native protein shows a single negative band centered at about 218 nm, which is characteristic of β-structure conformation (Sears & Beychok, 1973). We have performed an evaluation of the secondary structure content of the protein by computerized methods (Menéndez-Arias et al., 1988). Table I reports results obtained according to the method of Chang et al. (1978). The native protein features a large amount of β-structure. According to the analysis, the α-helix structure should be poorly organized with short helices ($n$ = 4). Bends and other structures are well represented. This result is consistent with the suggestion (Quax-Jeuken et al., 1985) that structural folding units of $\beta_s$-crystallin should be similar to those of $\gamma_2$-crystallin. The low intensity of the CD spectrum should poorly account for a reliable secondary structure analysis of the protein. However, the good fit renders the computed secondary structure content reasonably indicative of the structural organization. It should also be noted that other evaluation methods (Greenfield & Fasman, 1969; Bolotina et al., 1980, 1981; Brahms & Brahms, 1980) provide similar structural indications even if their fits were less acceptable from a statical point of view. We will discuss the pH effect later.

Figure 5 shows the near-UV circular dichroism spectra of the protein under the same experimental condition used to detect the dichroic activity in the far-UV. Ellipticity bands in the near-UV originate from the contribution of aromatic amino acid side chains (Strickland, 1974). At neutral pH, $\beta_s$-crystallin shows a positive peak essentially due to tyrosyl residues in the spectral range between 250 and 270 nm (Strickland, 1974). The shoulder at 264–265 nm might arise from the phenylalanine contribution (Strickland, 1974), which

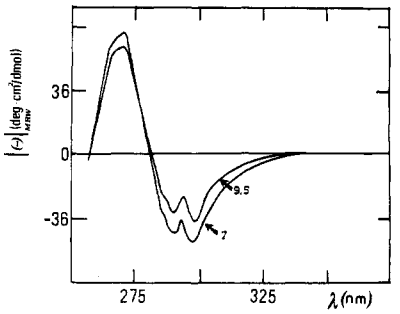


FIGURE 5: Near-UV CD spectra of $\beta_s$ at pH 7.0 and 9.5.

is not very evident in the near-UV CD spectrum or in the absorption spectrum of this protein. Contributions to the spectrum in the region from 275 to 300 nm have to be expected from tyrosine and tryptophan. At neutral pH, the CD spectrum shows two negative minima at 288 and 297 nm and a shoulder at 281–282 nm. These spectral features arise from overlaps of tyrosyl and tryptophanyl transitions (Strickland, 1974; Strickland et al., 1969). A correct assignment of these transitions lies beyond the boundaries of this study. However, the negative peak at 297 nm can be safely ascribed to tryptophan, while the minimum at 288 nm and the shoulder at 282 nm are due to the overlap of tryptophan and tyrosine transitions (Strickland et al., 1969; Strickland, 1974). It is also interesting to note that a weak negative CD band around 305–306 nm can be observed in the difference spectrum between near-UV CD spectra at pH 9.5 and 7 (not reported). This band might be ascribed to the presence of the $^1L_a$ vibronic band of tryptophan (Budzynski, 1971; Strickland, 1974).

*Effect of pH.* The structural stability of $\beta_s$-crystallin has been examined by following the effect produced by perturbing agents, such as guanidine hydrochloride and pH. Structural stability of $\beta_s$-crystallin to pH could not be studied at pH values lower than 6–6.5 because of coarse protein aggregation.

The far-UV CD spectrum of the protein at pH 9.5 is shown in Figure 4. In this condition, a decrease of dichroic activity is observed, although the spectrum still retains typical features of a $\beta$-structured protein. This observation is indicative of a pH-dependent structural change. The amounts of $\beta$, $\alpha$, and remaining structure of the protein at pH 9.5 as well as those calculated at neutral pH are reported in Table I.

A concomitant decrease of all peaks is also present in the near-UV CD spectrum of protein at pH 9.5, as shown in Figure 5. This observation indicates changes in the structural microenvironments surrounding all aromatic chromophores, i.e., in the tertiary structure. Therefore, both near- and far-UV measurements concomitantly suggest that the protein undergoes a pH-dependent transition.

Figure 6A reports both the pH dependence of tryptophanyl fluorescence at 330 and 350 nm (excitation at 295 nm) and far-UV CD at 208 nm. The fluorescence emission at 330 nm, characteristic of internal tryptophanyl residues, is quenched by raising the pH to 9.5. No fluorescence change is observed affecting the intensity at 350 nm, where exposed tryptophanyl residues emit. The shift of the fluorescence emission maximum and the fluorescence polarization are reported in Figure 6B. The emission maximum shifts from 322 to 333 nm, and the fluorescence polarization decreases from 0.16 to 0.10, thus indicating that the average tryptophan microenvironment becomes less compact and hydrophobic even if amino acid residues are still embedded into an organized structural matrix. In conclusion, the results indicate that the protein is stable only between pH 6.5 and 8. Above these values, a conformational change takes place in the pH 8–9.5 interval without a complete

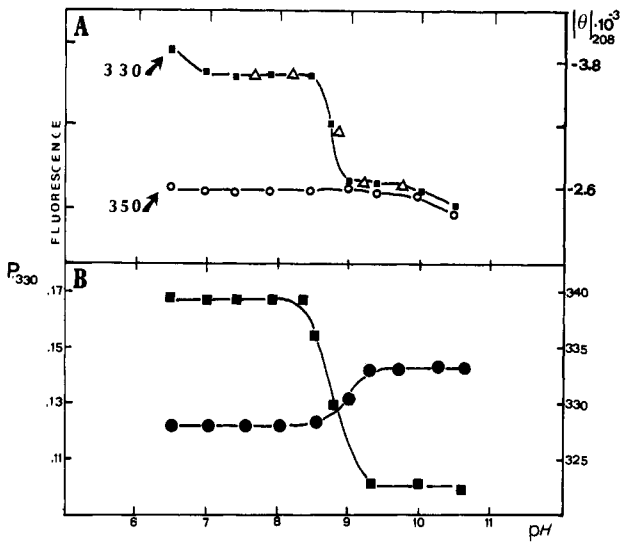


FIGURE 6: (A) pH dependence of $\beta_s$ fluorescence [emission at 330 (■) and 350 (○) nm] and far-UV CD ($[\theta]_{208}$) (△) in 0.05 M Tris-HCl and 0.15 M KCl. (B) pH dependence of $\beta_s$ fluorescence polarization (emission at 330 nm, excitation at 295 nm) (■) and emission maximum wavelength (excitation at 295 nm) (●) in 0.05 M Tris-HCl and 0.15 M KCl.

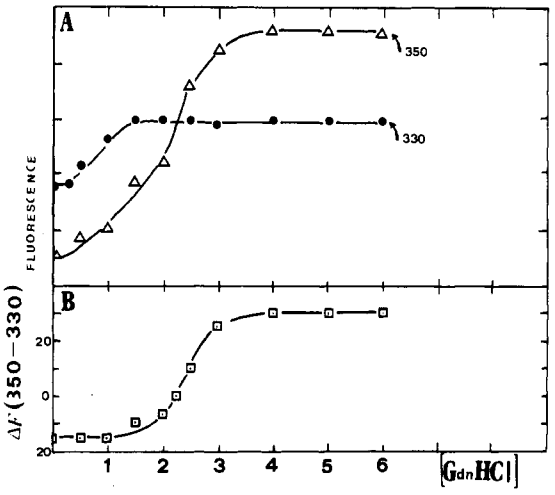


FIGURE 7: (A) Fluorescence emission at 330 and 350 nm (excitation at 295 nm) of $\beta_s$ versus GdnHCl concentration in the presence of 0.05 M phosphate and 0.15 M KCl. (B) Fluorescence difference curve (emission 350–330 nm) of $\beta_s$ versus GdnHCl concentration. Experimental conditions as in (A).

unfolding of the structure, as demonstrated by both fluorescence and circular dichroism measurements.

*Effect of GdnHCl.* The effect of increasing GdnHCl concentration on the structure of $\beta_s$-crystallin has been followed by numerous spectroscopic techniques. Results appear rather complex, probably reflecting the presence of structural domains. The unfolding transition can be considered partially reversible if care is taken to obtain a very slow and gradual refolding. The increase of denaturant concentration produces changes in both fluorescence intensity and emission maximum wavelength. Complete unfolding of the protein is observed only above 4 M GdnHCl, where both the emission maximum wavelength and fluorescence polarization assume the characteristic values of a fully unfolded polypeptide (350 nm and 0.05, respectively), which are very similar to those observed for low molecular weight model compounds in aqueous solution (Teale, 1960).

The dependence of tryptophan fluorescence on GdnHCl concentration is reported in Figure 7. We have followed

fluorescence intensity at 330 and 350 nm to discriminate the structural behavior of protein districts containing tryptophans. We must not forget that tryptophans-46 and -72 are deeply buried in the N-terminal part of the sequence (the first domain) and tryptophans-136 and -162 are located in the C-terminal part of the protein (the second domain). Tryptophan-136 is buried in the protein matrix, but tryptophan-162 is located in a very hydrophilic and flexible segment. The strategic location of the two groups of fluorophores should thus reflect the effect of denaturant on the whole structure of the protein as well as on the structural organization of each domain. Tryptophan microenvironments are already perturbed at low denaturant concentration. However, fluorescence intensity curves at 330 and 350 nm are far from being cooperative. Their increase with denaturant concentration also reveals that native tryptophans are located in structural environments where quenching effects of surrounding residues are relevant. The fluorescence emission at 330 nm does not increase above 1.5 M GdnHCl, while the emission at 350 nm increases up to 4 M GdnHCl.

An attempt made to understand the role of tryptophans is shown in Figure 7B. We have reported the fluorescence difference between intensities at 350 and 330 nm as a function of GdnHCl concentration. By considering that the change of protein fluorescence intensity at 350 nm should reflect the contribution of the most exposed tryptophanyl residue (i.e., Trp-162) and that the converse holds for the intensity at 330 nm, the intensity difference between 350 and 330 nm should be indicative of changes affecting the microenvironment of the exposed fluorophore. In fact, data show a denaturation curve that takes place from about 1.5 to 4 M GdnHCl. An increase of the fluorescence yield, due to the removal of some quenchers, is clearly evidenced. A close view at the structural environment of tryptophan-162 shows the presence of numerous residues as possible quenchers, i.e., Asp-152 and -161, Lys-153, -154, and -158, Glu-155, and Arg-157, only to mention the nearest sequence residues. The most important observation is that changes in the luminescence properties of the two major emitting classes of fluorophores occur as distinct processes. Internal chromophores exert their role prevalently at low denaturant concentration, between 0 and 1.5 M GdnHCl, whereas at higher denaturant concentration no further change is observed. The external fluorophore comes into play only at a denaturant concentration higher than 1.5 M.

Figure 8 shows the effect of denaturant concentration on the fluorescence emission maximum. The emission maximum of $\beta_s$-crystallin is linearly shifted to higher wavelengths from 1 to 4 M GdnHCl. The maximum is normalized to the solvent only at a denaturant concentration higher than 4 M. The denaturation effect takes place at low GdnHCl concentration according to fluorescence polarization measurements. The polarization increases slightly and then drops linearly from 0.17 to 0.07. At 3 M GdnHCl, the protein can be considered mostly denatured. A decrease of the polarization takes place down to 6 M GdnHCl, where the value of 0.05, a feature of freely rotating tryptophans, is slowly reached. This behavior probably reflects the presence of more relaxed structural states, which become progressively populated at higher denaturant concentration. The following points have to be stressed: (i) the presence of nonsuperimposable denaturation transitions; (ii) the wide concentration range necessary to unfold the protein; (iii) the consequent low cooperativity of curves. These observations indicate that we are dealing with a non-two-state process and with the probable presence of structural intermediates. Therefore, they confirm the presence of structural regions with independent unfolding pathways.

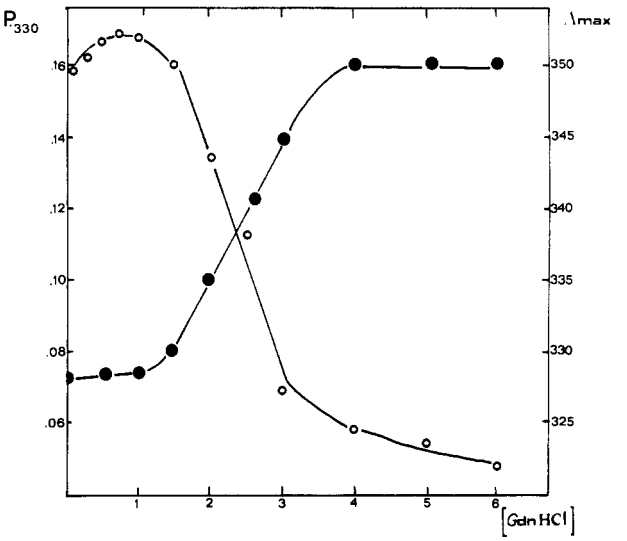


FIGURE 8: Fluorescence polarization at 330 nm (excitation at 295 nm) (○) and emission maximum wavelength (excitation at 295 nm) (●) of $\beta_s$ versus GdnHCl concentration. Experimental condition as reported in panel A of Figure 7.

## Discussion

In this study, we have estimated the structural organization of $\beta_s$-crystallin from calf lens in solution in order to assess its structural properties and stability. The main conclusions of our work are that (i) the protein possesses a very limited structural stability and (ii) its unfolding is not a two-state process. Its stability covers a very narrow range of experimental conditions (pH and strong denaturant). This finding could have important physiological implications. The range of pH stability spans only the region around neutrality, i.e., from pH 6.5 to 8. The protein precipitates after the pH is dropped to acid and undergoes a conformational change above pH 8, as well. Protonation (or deprotonation) of key residues is probably the driving force of these destabilizing effects in both circumstances. We suppose that changes in the protonation state of amino acid residues such as Glu and Asp might be the most probable reason for the precipitation in the acid pH region, while Cys and/or His might be involved in the conformational change of the alkaline region. Changes in the network of charge distribution are always a crucial factor of protein stability (Baker & Hubbard, 1984). The observation that a pH-induced conformational change is reflected by the fluorescence at 330 nm and that the fluorescence at 350 nm is not affected by pH suggests that mostly the N-terminal domain is involved in the alkaline pH transition.

In Figure 9, the net charge distribution of $\beta_s$- and $\gamma_2$-crystallin along their sequences is shown to find a reasonable structural explanation for the pH effect. Plots show a close similarity of charge distribution between the C-terminal domain of $\beta_s$-crystallin and the corresponding one of $\gamma_2$-crystallin. Moreover, differences exist between C- and N-terminal domains in both proteins. This difference was already recognized for $\gamma_2$-crystallin (Lindley et al., 1985). N-Terminal domains of $\beta_s$- and $\gamma_2$-crystallin also appear to be different between them. In fact, $\gamma_2$-crystallin shows a large cluster of positive charge in the first half of the sequence (from 10 to 70), while $\beta_s$ shows a rather uniform distribution of them. A large and deep negative minimum is centered around Cys-25 and -27 in $\beta_s$-crystallin. This region should correspond to a branch of the first motif if we assume a tertiary structure similarity between $\beta_s$ and $\gamma_2$. Numerous histidine (His-20 and -31) and aspartic acid (Asp-22, -24, -26, and -29) residues are also

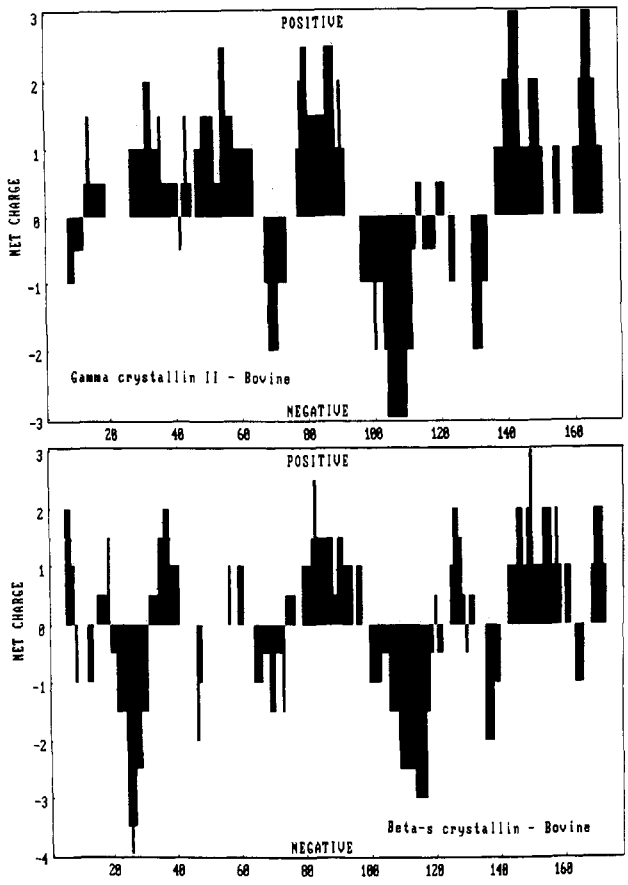


FIGURE 9: Plot of net charge distribution in $\beta_s$- and $\gamma_2$-crystallin along the sequence.

present in this segment, which is about 12 residues long. This cluster of charges can easily be altered by pH variations. The change of a negative net charge into a positive one may be the origin of the acid destabilization of native $\beta_s$, which induces the unfolding of the first motif of the N-terminal region. Deprotonation of both Cys-25 and -27 and of His-20 and -31 seems connected with the structural transition between pH 8 and 9.5 because of their p$K$'s. This sequence segment seems structurally relevant with respect to others in consideration of the high concentration of charged and protonatable groups. The conformational stability against a strong denaturant is another argument to evaluate the structural properties of a protein. It is well-known that the conformational stability of a protein is restricted and borderline and only accounts for few kilocalories per mole in the case of small globular proteins (Janin & Wodak, 1983; Jaenicke, 1987). Unfolding of $\beta_s$-crystallin by GdnHCl follows a rather complex mechanism, but from a stability–function point of view, it is important to note that unfolding starts at low concentration of denaturant. We will discuss the structural meaning of these observations later. Now, we would like to focus our attention on native molecule unfolding at low denaturant concentration. This suggests a very limited conformational stability for this protein. Therefore, if one considers that $\beta_s$-crystallin possesses a substantial limited stability and is weakly resistant to photochemical processes, we have a good candidate for some molecular pathways in eye lens pathologies. At present, its functional role is unfortunately unknown. It was stated that thermodynamic stability is a prerequisite for lens proteins because of their long life in the lens cell (Bloemendal, 1981; Maisel, 1985). Other authors (Wistow & Piatigorsky, 1987) also suggested that some crystallins could have been recruited during evolution as lens proteins because of their structural stability. These suggestions contrast with the very narrow range of $\beta_s$-crystallin stability, which is the main point of this work. The specific role of $\beta_s$ in the structure–function relationships of the lens supramolecular organization needs to be reexamined in light of our findings, which weaken previous hypotheses about the recruitment of crystallins as lens proteins. Of course, this observation does not rule out that the protein may have a prominent physiological role in the lens.

As far as the structural organization of $\beta_s$ is concerned, the protein shows a complex denaturation pattern. The wide range of denaturant concentration reasonably reflects the presence of overlapping structural transitions. This information also arises from the fluorescence behavior of internal and exposed tryptophans. The protein fluorescence is also complicated by emission heterogeneity. The fluorescence transition curves of $\beta_s$ at different emission wavelengths show that unfolding of the protein structure increases the quantum yield of tryptophan residues, which seem to be quenched by sterically related groups. The question arises whether the fluorescence reflects two distinct molecular transitions. The use of the fluorescence difference curve has clarified the behavior of the different emitting centers. The fluorescence emission of $\beta_s$ can be related to the presence of two structural domains on the ground of tryptophan location in the protein structure as suggested by predictive methods. Unfolding of the N-terminal domain should remove quenchers from blue-emitting tryptophans (46 and 76), as documented by the increase of fluorescence intensity observed between 0 and 1.5 M GdnHCl. Since Trp-162 should have its emission maximum centered at 330 nm, we must admit that the quantum yield increase upon unfolding of the C-terminal domain would predominantly depend on this fluorophore. Present data do not explain the role of Trp-136. This residue should be located close to the interdomain surface in analogy with $\gamma_2$-crystallin. It probably follows the fate of Trp-46 and -72 by reflecting the detachment of domains due to the unfolding of the N-terminal region.

The above-reported observation can be explained by assuming the presence in the $\beta_s$ molecule of two structural domains featuring two distinct unfolding transitions, having midpoints at 0.8 and at about 2.4 M GdnHCl, respectively. The two domains show quite a large difference of conformational stability, since the N-terminal domain is substantially less stable than the C-terminal one. Present data are unable to give an actual explanation for this effect because no apparent structural difference should exist between domains. A sequence inspection of $\gamma_2$ shows that amino acid variation between domains is high (Summers et al., 1984b). The network of interacting charges in the $\gamma$ fold also seems a crucial point of stability (Summers et al., 1984b). This indicates that the two domains may have different molecular properties. The charge distribution plots of $\beta_s$ and $\gamma_2$ (Figure 9) show that both proteins have dissymmetric charge patterns as far as their domains are concerned. Therefore, any agent altering the array of charges will weaken the structure. The high-salt effect of guanidine could play a specific role in the different way of destabilizing the two domains. It will be interesting to observe whether this peculiar difference of structural stability of $\beta_s$ is fulfilled by other members of the $\beta$ and $\gamma$ family.

## ACKNOWLEDGMENTS

We thank Dr. Joseph Sepe for critical reading of the manuscript.

## REFERENCES

Alcala, J., & Maisel, H. (1985) in *The Ocular Lens* (Maisel, H., Ed.) pp 169–222, Marcel Dekker, New York and Basel.

Baker, E. N., & Hubbard, R. E. (1984) *Prog. Biophys. Mol. Biol. 44*, 97–179.
Björk, I. (1964) *Exp. Eye Res. 3*, 254–261.
Bloemendal, H. (1981) *Molecular and Cellular Biology of the Eye Lens*, Wiley, New York.
Bolotina, I. A., Chekhow, V. O., Luganskas, V. Y., & Ptitsyn, O. D. (1980) *Mol. Biol. (Engl. Transl.) 14*, 709–715.
Bolotina, I. A., Chekhow, V. O., Luganskas, V. Y., & Ptitsyn, O. D. (1981) *Mol. Biol. (Engl. Transl.) 15*, 130–137.
Brahms, S., & Brahms, J. (1980) *J. Mol. Biol. 138*, 140–178.
Budzynski, A. J. (1971) *Biochim. Biophys. Acta 251*, 292–302.
Chang, C. T., Wu, C. C., & Yang, J. T. (1978) *Anal. Biochem. 91*, 13–31.
Chothia, C. (1984) *Annu. Rev. Biochem. 53*, 537–572.
Chou, P. V., & Fasman, G. D. (1974a) *Biochemistry 13*, 211–222.
Chou, P. V., & Fasman, G. D. (1974b) *Biochemistry 13*, 222–244.
Chou, P. V., & Fasman, G. D. (1978) *Adv. Enzymol. Relat. Areas Mol. Biol. 47*, 45–148.
Eftink, M. R., & Ghiron, C. A. (1976) *Biochemistry 15*, 672–680.
Facchiano, A. M., Facchiano, A., Facchiano, F., Ragone, R., & Colonna, G. (1989) *Comput. Appl. Biosci. 5*, 299–303.
Facchiano, F., Facchiano, A., Facchiano, A. M., Ragone, R., & Colonna, G. (1988) *Comput. Appl. Biosci. 4*, 303–305.
Greenfield, N., & Fasman, G. D. (1969) *Biochemistry 8*, 4108–4116.
Irace, G., Balestrieri, C., Parlato, G., Servillo, L., & Colonna, G. (1981) *Biochemistry 20*, 792–799.
Jaenicke, R. (1987) *Prog. Biophys. Mol. Biol. 49*, 65–87.
Janin, J., & Wodak, S. J. (1983) *Prog. Biophys. Mol. Biol. 42*, 21–78.
Lehrer, S. S., & Leavis, P. C. (1978) *Methods Enzymol. 49*, 222–236.
Lindley, P. F., Narebor, M. E., Summers, L. J., & Wistow, G. J. (1985) in *The Ocular Lens* (Maisel, H., Ed.) pp 123–167, Marcel Dekker, New York and Basel.
Maisel, H. (1985) in *The Ocular Lens* (Maisel, H., Ed.) pp 169–214, Marcel Dekker, New York and Basel.
Manavalan, P., & Ponnuswamy, P. K. (1978) *Nature 275*, 673–674.
Mandal, K., Chakrabarti, B., Thomson, J., & Siezen, R. J. (1987) *J. Biol. Chem. 262*, 8096–8112.
Menéndez-Arias, L., Gomez-Gutiérrez, J., Garcia-Fernandez, M., Garcia-Tejedor, A., & Moran, F. (1989) *Comput. Appl. Biosci. 4*, 479–482.
Pulcini, D., Stiuso, P., Miele, L., Della Pietra, G., & Colonna, G. (1989) *Biochim. Biophys. Acta 995*, 64–69.
Quax-Jeuken, Y., Driessen, H., Leunissen, J., Quax W., De Jong, W., & Bloemendal, H. (1985) *EMBO J. 4*, 2597–2602.
Ragone, R., Facchiano, F., Facchiano, A., Facchiano, A. M., & Colonna, G. (1989) *Protein Eng. 2*, 497–505.
Rose, G. D., Gierasch, L. M., & Smith, J. A. (1985) *Adv. Protein Chem. 37*, 1–109.
Sears, D. W., & Beychock, S. (1973) in *Physical Principles and Techniques of Protein Chemistry* (Leach, S. J., Ed.) Part C, pp 445–593, Academic Press, New York and London.
Siezen, R. J., & Argos, P. (1983) *Biochim. Biophys. Acta 748*, 56–67.
Siezen, R. J., Fisch, M. R., Slingsby, C., & Benedek, G. B. (1985) *Proc. Natl. Acad. Sci. U.S.A. 82*, 1701–1705.
Slingsby, C., & Croft, L. R. (1973) *Exp. Eye Res. 117*, 369–376.
Slingsby, C., & Miller, L. R. (1983) *Exp. Eye Res. 137*, 517–530.
Strickland, E. H. (1974) *CRC Crit. Rev. Biochem. 2*, 113–174.
Strickland, E. H., Horwitz, J., & Billups, C. (1969) *Biochemistry 8*, 3205–3213.
Summers, L., Slingsby, C., White, H., Narebor, M., Moss. D., Miller, L., Mahadevan, D., Lindley, P., Driessen, H., & Blundell, T. (1984a) *Ciba Found. Symp. 106*, 219–236.
Summers, L., Wistow, G., Narebor, M., Moss, D., Lindley, P., Sligsby, C., Blundell, T., Bartunik, H., & Bartels, K. (1984b) *Pept. Protein Rev. 3*, 147–168.
Tardieu, A., Laporte, D., Licinio, P., Krop, B., & Delaye, M. (1986) *J. Mol. Biol. 192*, 711–724.
Teale, F. W. J. (1960) *Biochem. J. 76*, 381–388.
Van Dam, A. F. (1966) *Exp. Eye Res. 5*, 255–260.
Wetlaufer, D. B. (1962) *Adv. Protein Chem. 17*, 303–390.
Wistow, G., & Piatigorsky, J. (1987) *Science 236*, 1554–1556.
Wistow, G., Slingsby, C., Blundell, T., Driessen, H., de Jong, W., & Bloemendal, H. (1981) *FEBS Lett. 133*, 9–16.
Wistow, G., Turnell, W. G., Summers L. J., Slingsby, C., Moss, D. S., Miller, L., Lindley, P. F., & Blundell, T. L. (1983) *J. Mol. Biol. 170*, 175–202.